


Article

# Rabbit as an Aging Model in Reproduction: Advanced Maternal Age Alters GLO1 Expression in the Endometrium at the Time of Implantation

Johanna de Nivelle \*, Juliane Thoma, Alicia Toto Nienguesso, Tom Seeling, Juliane-Susanne Jung , Anne Navarrete Santos and Maria Schindler \*

Institute for Anatomy and Cell Biology, Medical Faculty of Martin Luther University Halle-Wittenberg, 06108 Halle, Germany; thoma.juliane@gmx.de (J.T.); alicia.toto-nienguesso@medizin.uni-halle.de (A.T.N.); tom.seeling@medizin.uni-halle.de (T.S.); juliane-susanne.jung@medizin.uni-halle.de (J.-S.J.); a.navarrete-santos@medizin.uni-halle.de (A.N.S.)

\* Correspondence: johanna.de-nivelle@student.uni-halle.de (J.d.N.); maria.schindler@medizin.uni-halle.de (M.S.); Tel.: +49-345-557-4037 (J.d.N.); +49-345-557-1725 (M.S.)

Received: 29 September 2020; Accepted: 26 October 2020; Published: 31 October 2020



**Abstract:** Advanced maternal age is associated with adverse pregnancy outcomes and the decline of female fertility in mammals. A potential reason for reduced fertility is metabolic changes due to protein modifications by advanced glycation end products. To elucidate the aging process in female reproduction, we analysed a key enzyme for detoxification of reactive dicarbonyls, the glyoxalase 1 (GLO1), in reproductive organs and blastocysts of young and old rabbits at the preimplantation stage. At day 6 post coitum, uterine, oviductal, ovarian tissue and blastocysts from young (16–20 weeks) and old rabbits (>108 weeks) were characterised for GLO1 expression. GLO1 amounts, enzymatic activity and localisation were quantified by qPCR, Simple Western, activity assay and immunohistochemistry. The GLO1 enzyme was present and active in all reproductive tract organs in a cell-type-specific pattern. Ovarian follicle and uterine epithelial cells expressed GLO1 to a high extent. In tertiary follicles, GLO1 expression increased, whereas it decreased in the endometrium of old rabbits at day 6 of pregnancy. In blastocysts of old animals, GLO1 expression remained unchanged. In early pregnancy, advanced maternal age leads to modified GLO1 expression in ovarian follicles and the endometrium, indicating an altered metabolic stress response at the preimplantation stage in older females.

**Keywords:** preimplantation embryo; uterus; ovary; glyoxalase 1; advanced maternal age

## 1. Introduction

Over the past three decades there has been a pronounced increase in the number of births by older women, especially in their late 30s and 40s, in many high-income countries [1–3]. The mean age of women at birth of their first child has gradually increased from 27.0 in 1987 to 29.3 in 2018 in the European Union [4]. Women are evidently delaying childbearing. However, advanced maternal age can have detrimental effects on fertility and pregnancy outcome. It is well known that the developmental potential of oocytes declines with increasing age, referred to as ovarian aging. This phenomenon is characteristic not only for humans, but for all mammals [5–7]. Advanced maternal age is associated with a range of adverse pregnancy outcomes, including low birth weight, preterm birth and stillbirth [8–11]. It has been proposed that during the reproductive lifespan, ovarian follicles and reproductive tissues become exposed to factors that accumulate irreversibly, leading to an age-related decline of fertility [12,13].

Accumulation of harmful compounds such as advanced glycation end products (AGEs) is strongly associated with aging [14]. Furthermore, higher AGE levels correlate with aging-related diseases;

for example with diabetes, cancer and neurodegenerative diseases [15,16]. A major precursor of AGEs is the  $\alpha$ -oxoaldehyde methylglyoxal (MG), a dicarbonyl, which is physiologically formed during glycolysis, and to a lesser extent in cellular lipid and amino acid metabolism [17,18]. Dicarbonyl species are highly reactive, promoting posttranslational modifications of proteins, lipids and nucleic acids [19] and thus interfering with physiological functions of these molecules. MG reacts with arginine residuals to form argpyrimidine [20].

In physiological systems, defence against dicarbonyl glycation and particularly detoxification of MG mainly occurs via the glyoxalase system [21,22]. The glyoxalase system limits carbonyl stress toxicity [23]. It consists of two enzymes: the important rate-limiting glyoxalase 1 (GLO1) and glyoxalase 2 (GLO2, also known as hydroxyacyl glutathione hydrolase, HAGH) [24]. GLO1, the main component of the MG elimination system, is significantly decreased and associated with increased MG-AGEs in ovaries from mice with an advanced reproductive age in comparison to their young control group [25]. Moreover, studies have shown that AGEs are closely associated with female infertility and that AGE accumulation promotes ovarian oxidative stress and steroid hormone production, in consequence leading to ovarian dysfunction [26].

The reproductive dysfunction associated with aging has been so far characterised in terms of reduction of ovarian follicles and oocyte quality, as well as pregnancy complications (reviewed by Sauer [27]). While the extent of literature in this area is profound, there is currently limited knowledge on the molecular pathways leading to the impact that advanced maternal age has on the developmental competences of oocytes and embryos. We have recently shown that AGEs are present in ovarian tissues and embryos in rabbits [28]. Furthermore, the GLO1 enzyme is active in rabbit blastocysts as early as during preimplantation. The GLO1 amount decreases under pathophysiological conditions of maternal diabetes mellitus in embryos [29].

In the current study, we investigated the impact of maternal age on GLO1 expression and localisation in female reproductive organs and embryos at the preimplantation stage. For this purpose, we quantified GLO1 amounts and enzymatic activity of reproductive young (16–20 weeks) and old (over 108 weeks) rabbits in the uterus, oviduct and ovary, as well as in blastocysts on day 6 of pregnancy.

## 2. Materials and Methods

### 2.1. Animal Treatment and Recovery of Reproductive Tissues and Preimplantation Embryos

All animal experiments were performed in accordance with the principles of laboratory animal care and the experimental protocol had been approved by the local ethics committee (Landesverwaltungsamt Dessau; reference number: 42502-2-812).

To investigate whether the glyoxalase system changes with maternal age in reproductive organs during the preimplantation stage, we examined the ovaries, oviduct and uterus of rabbits on day 6 of pregnancy. At least nine young rabbits (16–20 weeks), equivalent to young fertile women, and 13 old rabbits (108–172 weeks), equivalent to 40-years-old women, were analysed for GLO1 expression, activity and localisation. Sexually mature rabbits (New Zealand White, hybrid strain Zika, acquired from Dr. Zimmermann GbR, Germany) were maintained under species-appropriate conditions for four weeks before mating. Female rabbits were mated with two fertile bucks. No hormonal stimulation was used. On day 6 post coitum (p.c.), rabbits were sacrificed using a lethal dose of pentobarbital and reproductive tissues, such as ovary, oviduct and uterus, were collected.

Ovarian, oviductal and uterine tissue sections were prepared and stored at  $-80^{\circ}\text{C}$  until usage for RNA and protein isolation or in bouin<sup>®</sup> fixation solution (Sigma Aldrich, Taufkirchen, Germany) for immunohistochemistry. Uterine endometrium was abraded mechanically from the myometrium and stored at  $-80^{\circ}\text{C}$  before RNA and protein isolation.

Six-day-old blastocysts were flushed from the uterus, washed three times with PBS and characterised morphologically. On day 6 p.c., gastrulation stage of blastocysts was determined

under the stereomicroscope according to morphological characteristics of the embryonic disc which is summarised by Fischer et al. [30].

Blastocysts at the pre-gastrulating stage 0 with no apparent axial differentiation in the embryonic disc were used for analysis. Embryonic coverings were mechanically removed under a stereomicroscope. Blastocysts were stored at  $-80^{\circ}\text{C}$  until use for RNA and protein isolation.

## 2.2. RNA Isolation and cDNA Synthesis of Reproductive Tissues

Total RNA extraction from ovary, oviduct and endometrium tissue was performed using TRI Reagent<sup>®</sup> (Sigma-Aldrich, Taufkirchen, Germany) according to described protocol [31]. The amount of total RNA was measured spectrophotometrically at 260 nm. To check RNA quality, 260/280 ratio was calculated. Seven  $\mu\text{g}$  of isolated mRNA were treated with 4 U DNase-free<sup>™</sup> Kit (Invitrogen, Darmstadt, Germany) for 30 min at  $37^{\circ}\text{C}$ . As a control for remaining DNA contamination, 1  $\mu\text{g}$  RNA was PCR amplified without reverse transcription reaction.

One  $\mu\text{g}$  of DNA-free RNA was transcribed into cDNA using 200 U reverse transcriptase (RevertAid H Minus RT, Thermo Scientific, USA) and random primer (p(dN)<sub>6</sub>, Roche, Basel, Switzerland) at  $42^{\circ}\text{C}$  for 1 h, followed by incubation at  $70^{\circ}\text{C}$  for 10 min.

## 2.3. RNA Isolation and cDNA Synthesis of Single Blastocysts

Messenger RNA (mRNA) of single blastocysts was extracted with Dynabeads<sup>®</sup> Oligo (dT)25 (Invitrogen, Darmstadt, Germany). Blastocysts were lysed in 20  $\mu\text{L}$  lysis buffer (100 mM Tris/HCl pH 7.5, 500 mM LiCl, 10 mM EDTA pH 8, 0.1% SDS). Blastocyst lysate was hybridised with 5  $\mu\text{L}$  Dynabeads for 5 min and separated by magnetic adhesion for 2 min. The supernatant was removed and the pellet was washed as described in Tonack et al. [32]. Isolated mRNA was resolved in 11  $\mu\text{L}$  DEPC and total mRNA amount was used for cDNA synthesis. Water was added for a final cDNA reaction volume of 100  $\mu\text{L}$ .

## 2.4. Measurement of mRNA Levels by Quantitative PCR

For GLO1 the amplification and quantification forward (5'-ACCCAGCACCAAGGATTTT-3') and reverse primer (5'-GTGCCCCAATTGTGTGTCAG-3') were designed based on the rabbit GLO1 gene sequence (Gene ID: 100,354,439 NCBI, accession number: XM\_002714686) by Primer-BLAST. PCR products were sequenced and checked for specificity as described previously by Seeling et al. [29].

Quantitative PCR (qPCR) analyses were performed in duplicates using the Quant Studio 3<sup>™</sup> Real Time System (ThermoFisher, Schwerte, Germany) with no template controls for each primer set. QPCR runs were performed on 3  $\mu\text{L}$  cDNA with 17  $\mu\text{L}$  MasterMix (PowerTrack<sup>™</sup> SYBR Green Master Mix, ThermoFisher, Schwerte, Germany). Vinculin was simultaneously quantified as the endogenous control. The target gene expression was normalised to that of vinculin in each sample. Forward (5'-CCGTGAGGCTGGTTACGC-3') and reverse primer (5'-CGGGCAACAGAGAACTAGGAA-3') were designed based on the rabbit vinculin gene sequence (Gene ID: 100,357,160 NCBI, accession number: XM\_002718406.3). For quantification, GLO1 and vinculin calibration curves were included from serial dilutions ( $10^7$ – $10^3$  copies) of gene specific DNA plasmid standards. Quantification of mRNA amount was calculated using a comparative method ( $\Delta\Delta\text{CT}$ ). The threshold cycle (CT) for each gene was normalized to vinculin (house-keeping gene) and expressed as relative to the mean of the young control group.

## 2.5. Protein Preparation and Immunoblotting

Embryonic proteins and tissue samples were isolated as previously described [33,34]. Tissues were homogenized in 500  $\mu\text{L}$  of cold radio immunoprecipitation assay (RIPA) buffer with protease and phosphatase inhibitor (Roche, Basel, Switzerland). In one embryonic protein sample, 5–13 blastocysts were pooled. For analysis 4 samples from young and 6 from old rabbits were used.

The Simple Western™ method was used for GLO1 protein analysis and carried out in accordance to the manufacturer's instructions. This method enables automated size-based separation of protein samples with subsequent immunoblotting within provided capillaries. In an initial step, the extracted denatured protein samples (0.4 µg/µL tissues and 0.6 µg/µL blastocysts), primary antibodies, horseradish peroxidase (HRP) conjugated secondary antibodies, and the detection-mix were dispensed on a 384-well microplate. An overview of the used antibodies is shown in Table 1. A detailed description of the assay plate design and method is provided in the supplemental (Figures S1 and S2). For peak identification, electropherograms were used, which can be digitally converted into traditionally looking blots (Figure S3). Blots of Simple Western data are provided in the supplemental (Figures S5–S8). Compass software was used to process and analyse all data results. The protein amount was calculated as the ratio of area under the curve (GLO1 protein vs. vinculin) in the same run to correct for differences in protein loading.

**Table 1.** List of primary and secondary antibodies used for the Simple Western™ method.

Antigen	Name of Antibody	Manufacturer/Company Catalogue NO.	Type	Dilution
GLO1	GLO1 (D-5)	santa cruz, sc-133214	MM	1:50
Vinculin	Vinculin (7F9)	santa cruz, sc-73614	MM	1:300
Mouse IgG	Peroxidase-conjugated AffiniPure Donkey anti-mouse IgG (H + L)	Jackson ImmunoResearch, 715-035-150	DP	1:300
Mouse IgG	Secondary HRP Conjugate Goat anti-mouse IgG (H + L)	ProteinSimple, 042-205	MP	undiluted

MM: mouse monoclonal; DP: donkey polyclonal, MP: mouse polyclonal.

## 2.6. GLO1 Enzymatic Assay

The activity of GLO1 was measured spectrophotometrically in accordance with Bélanger et al. [35]. A total amount of 10 µg isolated protein per sample were loaded onto an UV microplate (Corning Inc., Corning, NY, USA) and 200 µL of reaction mix was added, as previously described in Seeling et al. [29]. The change in absorbance ( $\Delta E$ ) at 240 nm was measured every minute for one hour at 37 °C, to allow the reaction to reach saturation. GLO1 activity was calculated using  $\Delta E$  in the linear range after correction for blank:  $A = (V_{\text{total}} \times \Delta E) / (V_{\text{sample}} \times \epsilon_{\text{hemithioacetal}} \times d)$ , with  $\Delta \epsilon_{240} = 2.86 \text{ mM}^{-1} \cdot \text{cm}^{-1}$  [36]. Specific GLO1 activity was calculated as a ratio of relative GLO1 activity and GLO1 protein amount within the same sample.

## 2.7. Immunohistochemical Localisation of GLO1 and Argpyrimidine in the Reproductive Tract Organs

Ovarian, oviductal and uterine tissues were prepared as described in Haucke et al. [28]. Endogenous peroxidases were inhibited by incubating the slides with 3% H<sub>2</sub>O<sub>2</sub> in Methanol for 25 min. After blocking with 10% goat serum for one hour, the slides were incubated with mouse monoclonal antibody against GLO1 (1:200, #133214, Santa Cruz, Santa Cruz, CA, USA) or argpyrimidine (1:100, Biologo, Kiel, Germany) diluted in 1% (wt/vol) BSA/PBS at 4 °C overnight. For detection, the secondary antibody Dako EnVision + System-HRP labelled Polymer anti-mouse (1:1 in PBS; Dako, Jena, Germany) and diaminobenzidine (DAB; WAK-Chemie Medikal, Steinbach, Germany) were used. As negative control, the control reaction of the HRP-conjugated secondary goat anti-mouse IgG without the primary antibody was used. The DAB reaction was stopped after 4–6 min. Nuclei were counterstained blue with haematoxylin for 5 min. All steps were performed within the same experiment, examined microscopically during the same session, using an identical microscope (Leica DMi8, Wetzlar, Germany) and camera settings. Description of immunohistochemical evaluation is provided in the supplemental (Figure S4). The software Leica Application Suite X was used for image acquisition and editing.

## 2.8. Statistics

Statistical analysis was performed using OriginPro 2019 software (OriginLab Corporation, Northampton, MA, USA). Student's t-test or one-way ANOVA was used after proving normal distribution. Mann–Whitney U test was used, if normal distribution could not be proven. For results displayed as box plots, the white squares show the mean values. Median values are represented by a black line. The upper/lower whisker represents  $Q1/Q3 \pm 1.5 \times$  interquartile range. Results shown by bar chart are expressed as mean value  $\pm$  standard error of the mean (mean  $\pm$  SEM). Levels of significance are labelled as follows: \*  $p < 0.05$ , \*\*  $p < 0.01$ . ( $n$ ) represents the number of samples used for the measurement per group, ( $N$ ) the number of animal experiments from which embryonic samples were recovered.

## 3. Results

### 3.1. Expression and Activity of GLO1 in the Ovary of Young and Old Rabbits on Day 6 of Pregnancy

In ovary samples from young and old rabbits, comparable amounts of GLO1 transcripts, GLO1 protein and GLO1 activity were measured (Figure 1).

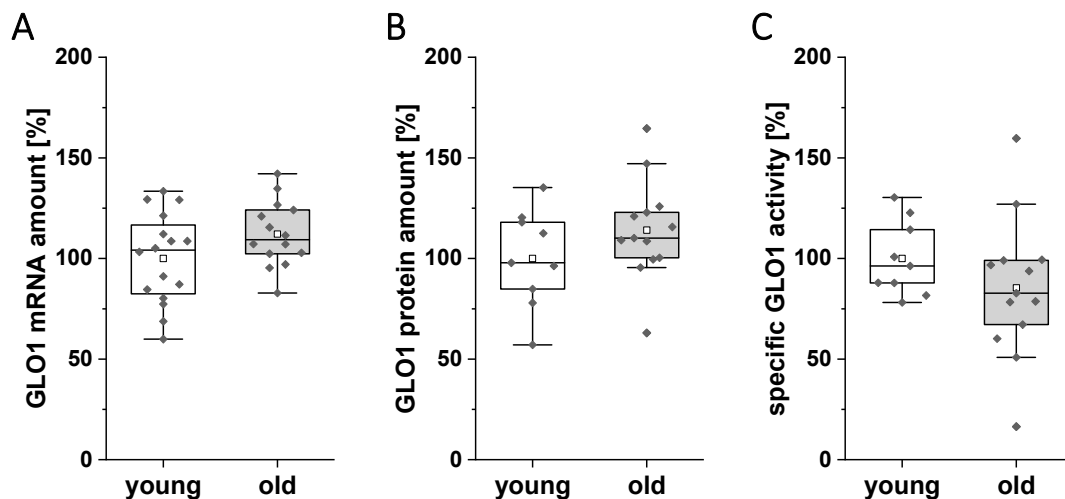


**Figure 1.** Quantification of GLO1 mRNA, protein and enzymatic activity in the ovary of young and old rabbits at day 6 p.c. (A) GLO1 mRNA levels were quantified by qPCR. (B) GLO1 protein was measured by the Simple Western method. Both mRNA and protein amount were normalised to the levels of vinculin. (C) Enzymatic GLO1 activity was measured spectrophotometrically in 10  $\mu$ g ovarian protein lysate. Specific GLO1 activity was calculated relative to GLO1 protein amount within the same sample. Results are shown as box plots. All values are expressed in per cent, with young rabbits = 100% ( $n \geq 9$ ).

Immunohistochemical staining of the ovary revealed that in young and old rabbits GLO1 was exclusively localised in the cytosol and nucleoplasm, showing a dominant staining in follicles in the oocyte and the surrounding follicular epithelium, as well as the germinal epithelium (Figure 2A). During follicle maturation, the follicular cells differentiate to become several layers of granulosa cells, which showed the most prominent GLO1 staining. Ovarian stromal cells and the theca folliculi showed weaker staining. In the ovaries of old rabbits, tertiary follicles were more intensively stained than those of young ones (Figure 2C), indicating an increased expression of GLO1 at this follicle stage in old animals.



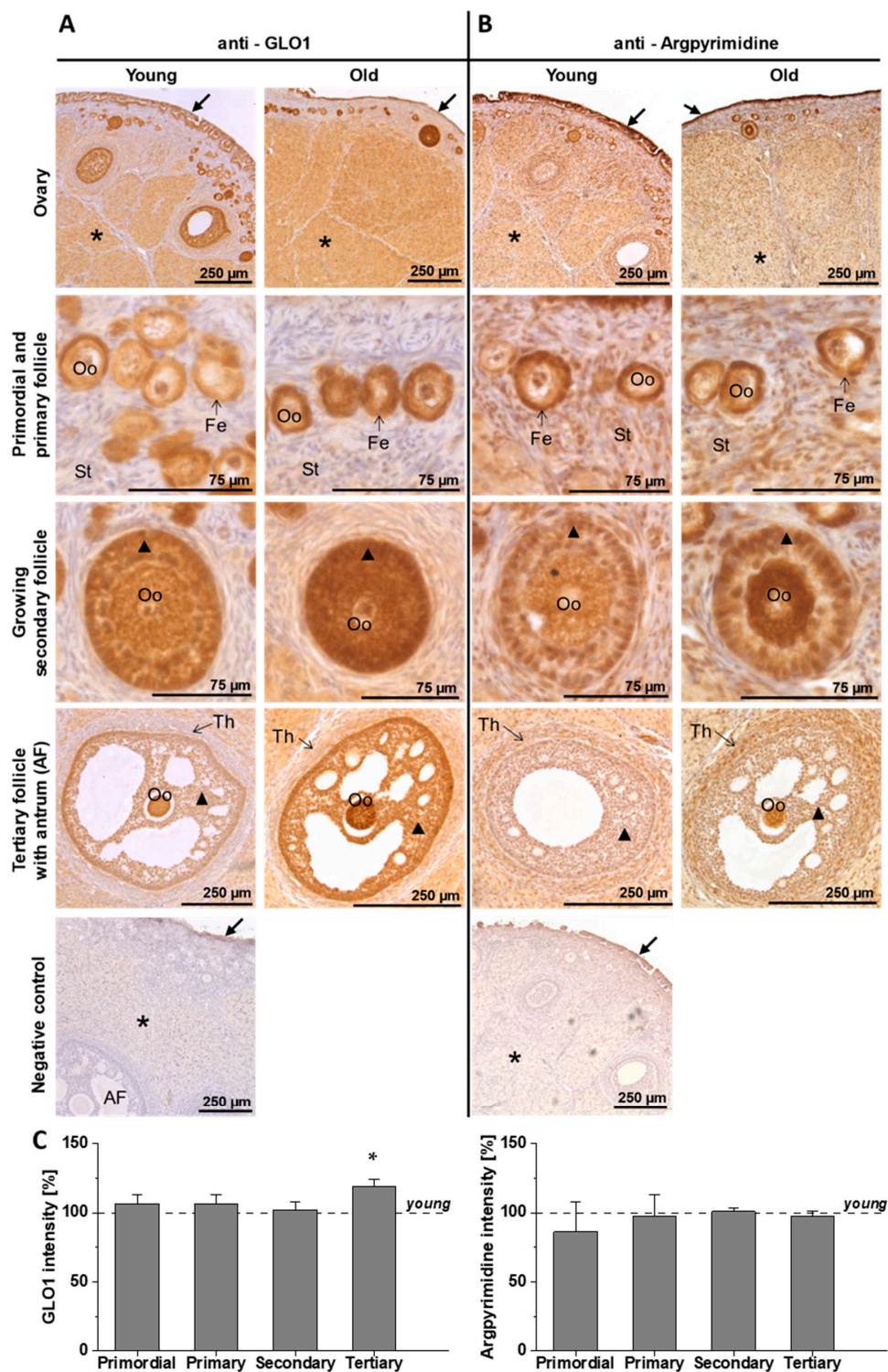


**Figure 2.** Immunohistochemical analysis of GLO1 (A) and argpyrimidine (B) in the ovary of young and old rabbits. GLO1 and argpyrimidine were visualised through a peroxidase–diaminobenzidine reaction (brown colour). Nuclei were stained with haematoxylin (blue colour). Oo = Oocyte. Th = Theca folliculi. St = Stromal cells. Fe = Follicular epithelium. → = Germinal epithelium. ▲ = Granulosa cells. \* = Corpus luteum. (C) GLO1 and argpyrimidine staining intensities were evaluated independently and blindly by at least two researchers. Staining was graded using a scale from 0 (none) to 5 (very strong). The diagram depicts the staining intensity by follicle stage, calculated as average of oocyte, follicular epithelium/granulosa cell and theca folliculi grading. Relative intensities are expressed as mean ± SEM in per cent, with young rabbits = 100% ( $n = 6$ ; \*  $p = 0.012$ ).

The AGE argpyrimidine was colocalised in ovarian sections from young and old rabbits (Figure 2B). For argpyrimidine, immunohistochemical analysis revealed a cytosolic as well as a nucleoplasmatic localisation, particularly in stromal cells, corpus luteum and theca folliculi. Staining patterns were similar to those of GLO1, with the strongest signal being observed in the follicles. Comparing argpyrimidine staining to that of GLO1 at the tertiary stage, a more distinct staining was found in the theca folliculi, while granulosa cell staining was reduced. At all follicle stages, no differences in argpyrimidine distribution between young and old rabbits were observed (Figure 2C).

### 3.2. Expression and Activity of GLO1 in the Oviduct of Young and Old Rabbits on Day 6 of Pregnancy

In mammals, fertilisation takes place in the oviduct. Local changes in reactive dicarbonyls may have a long-term impact on the developing embryo. As an indicator for possible changes, we analysed the expression of GLO1 in the oviduct. GLO1 expression and activity were not altered in the oviduct of old rabbits (Figure 3A–C).

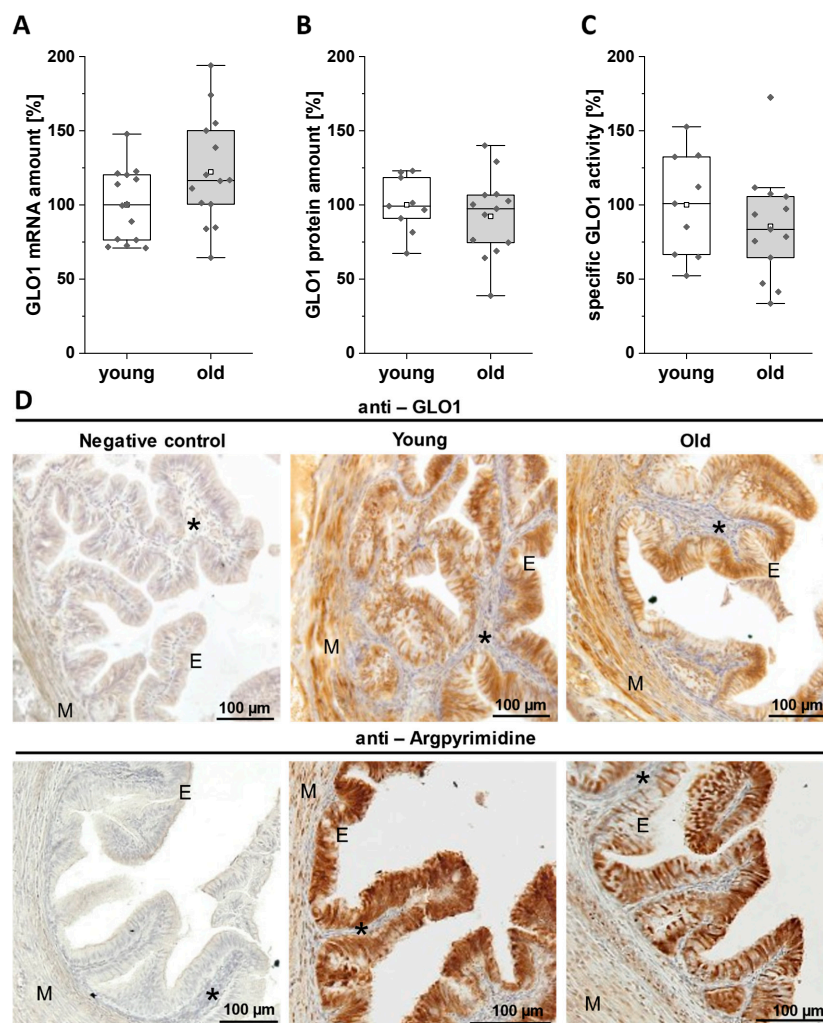


**Figure 3.** Quantification of GLO1 mRNA, protein and enzymatic activity in the oviduct of young and old rabbits at day 6 p.c. (A) GLO1 mRNA levels were analysed by qPCR. (B) GLO1 protein analysis was carried out by Simple Western method. Vinculin was used for normalization to calculate relative mRNA and protein amounts. (C) Enzymatic GLO1 activity was measured spectrophotometrically in 10 µg oviductal protein. Specific GLO1 activity was calculated relatively to GLO1 protein amount within the same sample. Results are shown as box plots. All values are expressed in per cent, with young = 100% ( $n \geq 9$ ). (D) Immunohistochemical analysis of GLO1 and argpyrimidine in cross-sections through the oviduct. M = Muscularis. \* = Mucosa layer with (ciliated) columnar epithelium (E).

We further analysed the localisation of GLO1 and the AGE argpyrimidine in the oviduct of young and old rabbits (Figure 3D). GLO1 was localised in the cytosol and nucleoplasm. An intense staining was revealed in the oviductal epithelium with secretory and ciliated cells, as well as the muscularis layer. Furthermore, smooth muscle cells from vessels were stained positive for GLO1. In oviducts of young and old rabbits, no differences in GLO1 staining, neither in localisation nor in intensity, were observed. Argpyrimidine showed a cytosolic as well as a nucleoplasmatic localisation, particularly in the oviductal epithelium and the muscularis layer. Staining patterns were similar to those of GLO1. No differences in argpyrimidine localisation between young and old rabbits were observed.

### *3.3. Expression and Activity of GLO1 in the Uterus of Young and Old Rabbits on Day 6 of Pregnancy*

The uterus, especially the endometrium, are crucial organs for embryo implantation and the establishment of a successful pregnancy. We analysed the GLO1 expression and activity in the pregnant uterus at day 6 p.c. In the endometrium of old rabbits, we observed significant lower GLO1 mRNA and protein levels (Figure 4A,B), whereas the specific GLO1 activity was not altered (Figure 4C).

In the uterus, GLO1 was localised in the myometrium, as well as in the glands and epithelium of the endometrium. The stroma of the endometrium was weakly stained. No differences in GLO1 localisation and staining intensity were observed between young and old rabbits (Figure 4D). The GLO1 protein decrease detected by qPCR and Simple Western (Figure 4A,B) was not evident in immunohistochemical sections.

For the AGE argpyrimidine, immunohistochemical analysis showed a cytosolic as well as a nucleoplasmatic localisation, particularly in the myometrium, glands and epithelium. In contrast to GLO1, argpyrimidine was also localised in stromal cells. Comparing the staining pattern to that of GLO1, the argpyrimidine staining showed more variety across the endometrium, with a very intense staining in some distinct endometrial cells. In the endometrium of old rabbits, more of these intensively stained endometrial cells were detected than in young rabbits (Figure 4D), indicating an increased accumulation of argpyrimidine in the endometrium of old animals.



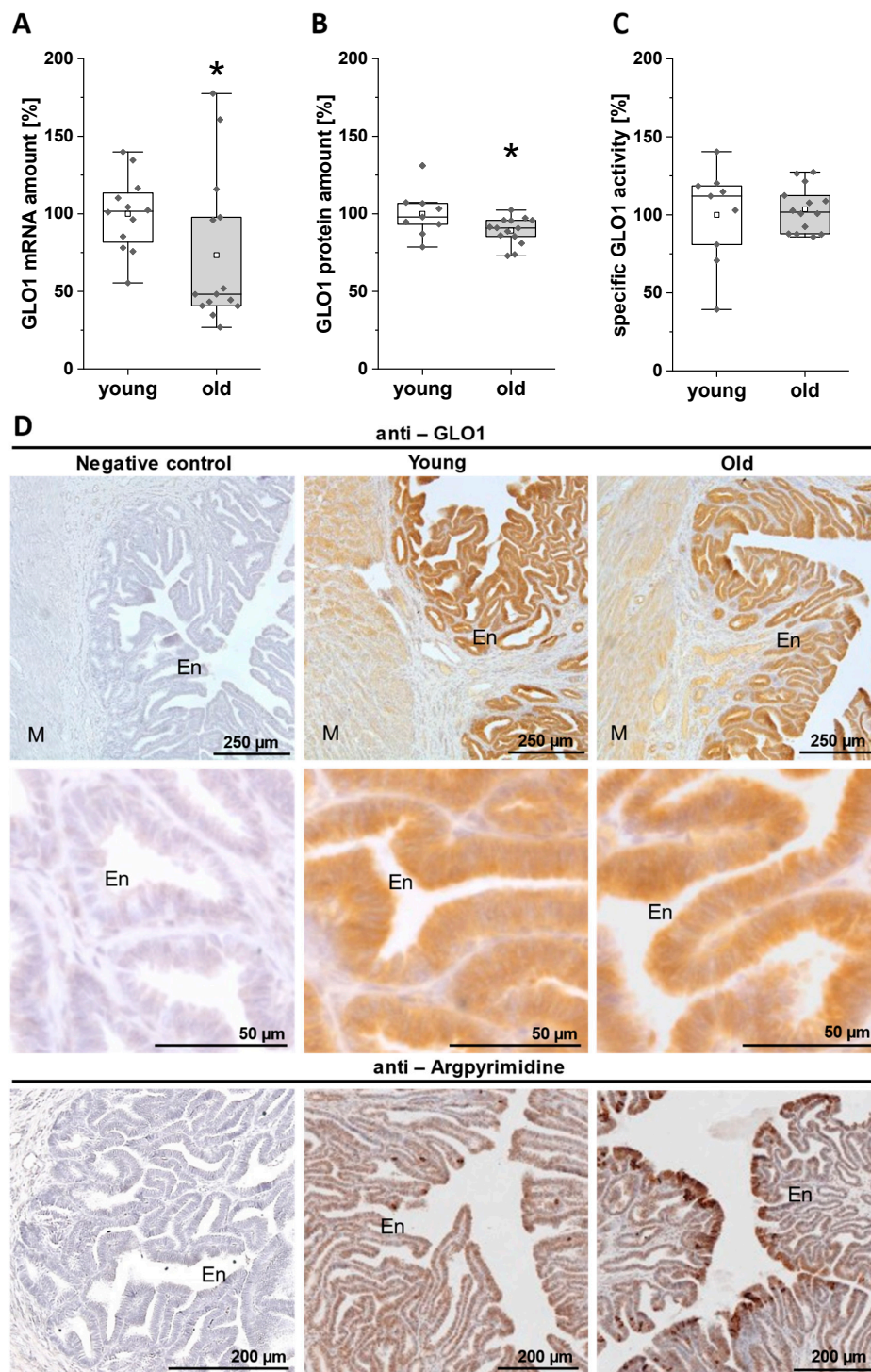


**Figure 4.** Quantification of GLO1 mRNA, protein and enzymatic activity in the endometrium of young and old rabbits at day 6 p.c. (A) GLO1 mRNA levels were quantified by qPCR. The Mann–Whitney U test was used for statistical analysis (\*  $p = 0.033$ ). (B) GLO1 protein analysis was carried out by the Simple Western method. Relative mRNA and protein amount are normalised to the levels of vinculin (\*  $p = 0.038$ ). (C) Enzymatic GLO1 activity was measured spectrophotometrically in 10  $\mu\text{g}$  endometrial protein. Specific GLO1 activity was calculated relatively to GLO1 protein amount within the same sample. Results are shown as box plots. All values are expressed in per cent, with young = 100% ( $n \geq 9$ ). (D) Immunohistochemical detection of GLO1 and argpyrimidine in cross-sections through the uterine wall. M = Myometrium. En = Endometrium.

### 3.4. mRNA and Protein Amount of GLO1 in Blastocysts of Young and Old Rabbits on Day 6 of Pregnancy

In blastocysts from old rabbits, GLO1 mRNA amount was not altered (Figure 5A). On protein level, the mean value of the GLO1 quantity was higher in embryos from old animals; however, the difference did not reach statistical significance (Figure 5B).

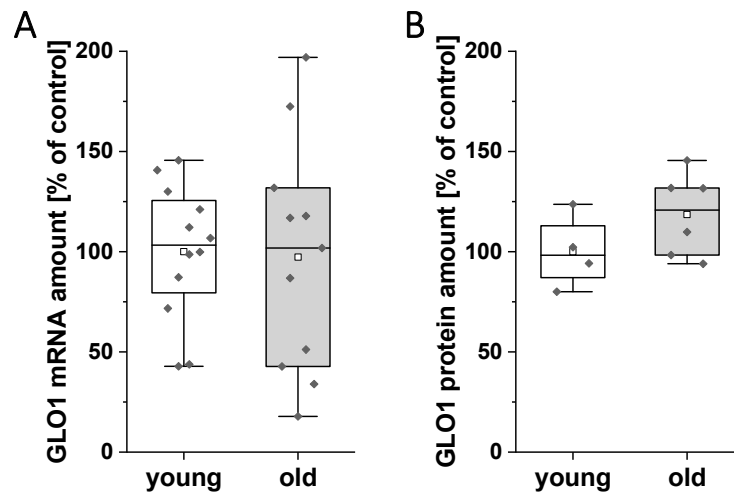


**Figure 5.** Quantification of GLO1 mRNA and protein amount in 6-day old blastocysts from young and old rabbits. (A) GLO1 mRNA levels were quantified by qPCR. ( $N = 2, n \geq 11$ ) (B) For GLO1 protein analysis by the Simple Western method pooled embryonic samples with 5–13 blastocysts were used ( $N = 2, n \geq 4$ ). Results are shown as box plots. Relative mRNA and protein amount are normalised to the levels of vinculin. All values are expressed in per cent, with young = 100%.

## 4. Discussion

The postponement of childbearing to the fourth decade of life has made reproductive aging a central topic that entails negative consequences for individual fertility and pregnancy outcome but also for society. Reproductive organs are exposed to metabolites that irreversibly accumulate during the reproductive lifespan, including compounds such as AGEs [25]. The main precursors of AGEs are reactive dicarbonyls, such as MG.MG, which is a ubiquitous reactive dicarbonyl that is eliminated by the glyoxalase system [18,21]. However, some reactive dicarbonyls can escape detoxification and react to form stable AGEs. The accumulation of reactive dicarbonyl compounds can be caused by decreased elimination or increased formation. In the current study, we focused on the key enzyme of the detoxification system, GLO1, in reproductive tissues and embryos of old and young rabbits.

GLO1 represents the frontline defence against dicarbonyl glycation in physiological systems, limiting dicarbonyl stress [21,22]. We could show that GLO1 is expressed in the ovary, oviduct, uterus and blastocyst of rabbits. We observed lower levels of GLO1 in the endometrium of old rabbits whilst the specific GLO1 activity remained the same, implicating an absolute decrease of GLO1 activity in this tissue. In the ovary of polycystic ovary syndrome (PCOS) rats, AGEs lead to reduced GLO1 [37]. In the immunohistochemical analysis of the uterus we observed an increased accumulation of the AGE argpyrimidine in endometrial cells of old rabbits. The decreased amount of GLO1 in the endometrium may be caused by higher AGE levels in the uterine environment of old rabbits. Our findings indicate an impaired AGE defence and higher exposure to dicarbonyl stress in endometrial cells—the cell layer that directly forms and interacts with the surrounding milieu of the developing blastocyst.

The importance of GLO1 has been shown in several knock down studies. The lack of GLO1 in cell culture and animal models results in increased levels of free MG and MG-derived AGEs [38,39]. GLO1 activity is inversely correlated to elevated levels of AGEs and androgen levels, in consequence leading to hormonal imbalance [37]. Hormonal imbalance can impair fertility and pregnancy establishment, as observed in women with advanced maternal age [40]. Lower levels of GLO1

in the endometrium may indicate higher AGE levels and oxidative stress in the uterine cavity fluid, the surrounding milieu of the developing embryo. We have shown already that AGEs such as argpyrimidine, CML and pentosidine are present in rabbit blastocysts [28]. Further research is needed to analyse whether oxidative stress and the levels of AGEs are increased in the blastocysts of old rabbits.

In humans, AGE-modified proteins were detected in follicular cell layers, granulosa and theca cells and in luteinised cells, with a more prominent staining in granulosa cells of women with PCOS [41]. In PCOS patients, AGEs are able to modulate extracellular matrix organisation, leading to deregulation of folliculogenesis [42]. Increased MG and AGE levels, paired with a lower GLO1 expression, resulted in ovarian proteome damage in the mouse model [25]. Accumulation of AGEs in the ovary may, therefore, be one reason for the impaired folliculogenesis in women with an advanced maternal age [43]. A possible correlation between AGEs and follicle aging was first described by an observational study. They could show that the AGE pentosidine was increased in the primordial, primary and atretic follicles of postmenopausal women [44]. In rabbit ovaries, we observed that the AGE argpyrimidine accumulates in follicular cells, especially in granulosa cells. The coincidence of argpyrimidine and GLO1 indicates a high metabolic stress level in these specific cells. As mentioned above, in human ovary AGEs accumulate in follicles with an advanced maternal age. Changes of GLO1 in the reproductive organs and a possible interaction with AGEs are likely in humans as well. However, the rabbit reproductive model only reflects human development during blastocyst formation. Accordingly, results are limited to the developmental stages investigated. Another limitation of the current study is its sole focus on the anti-glycation enzyme GLO1. Other anti-glycation enzymes, such as aldehyde dehydrogenase or aldose reductase, could be investigated in further studies.

In this observational study GLO1 expression and AGE levels were described and quantified. The functional relationships and regulations between increased AGEs and decreased GLO1 amounts were not investigated. A recently published study could show that SIRT1 participates in modulation of MG scavenging in mouse oocytes by promoting the expression of GLO1, SOD2 and catalase to avoid ovarian AGE accumulation [45]. These antioxidant enzymes play a role in the defence system of the ovary [46] and uterus [47] and could give further understanding of GLO1–AGE interactions in the aged endometrium.

## 5. Conclusions

In rabbits, an advanced maternal age reduces GLO1 expression in the endometrium at the time of implantation, indicating a decrease of metabolic stress defence in the aging uterus. We suppose that a modified GLO1 expression can be one mediating factor regarding the age-related decline in pregnancy rate. Further research is needed to expand analysis of AGEs–GLO1 interactions on a molecular level and the consequences for early embryo–maternal communication.

**Supplementary Materials:** The following are available online at <http://www.mdpi.com/2076-3417/10/21/7732/s1>. Figure S1: Assay plate design for Simple Western; Figure S2: Simple Western method, modified after ProteinSimple [48]; Figure S3: Example of Simple Western run analysis; Figure S4: Immunohistochemistry grading; Figure S5: Simple Western of the ovary; Figure S6: Simple Western of the oviduct; Figure S7: Simple Western of the endometrium; Figure S8: Simple Western of blastocysts.

**Author Contributions:** Conceptualization, A.N.S., M.S., J.d.N.; methodology: A.N.S., M.S., J.-S.J., T.S.; validation: M.S., A.N.S.; formal analysis: J.d.N., M.S., A.T.N.; investigation: J.d.N., M.S., A.T.N., J.T.; resources: J.d.N., J.T., T.S., A.T.N., M.S., A.N.S., J.-S.J.; data curation: J.d.N., J.T.; writing—original draft preparation: M.S., J.d.N.; writing—review and editing: M.S., A.N.S., J.D.N., A.T.N., J.-S.J., J.T.; visualization: J.D.N., M.S.; supervision: M.S., A.N.S.; project administration: A.N.S., M.S.; funding acquisition: A.N.S., M.S. All authors have read and agreed to the published version of the manuscript.

**Funding:** This work was supported by the German Research Foundation GRK 2155. The funders had no role in study design, data collection and analysis, decision to publish, or preparation of the manuscript.

**Acknowledgments:** We thank Sabine Schrötter and Jennifer Kopietz for excellent technical assistance. We acknowledge the financial support within the funding programme Open Access Publishing by the German Research Foundation (DFG) and the ZMG for providing access to SallySue.

**Conflicts of Interest:** The authors declare no conflict of interest.

## References

1. Huang, L.; Sauve, R.; Birkett, N.; Fergusson, D.; van Walraven, C. Maternal age and risk of stillbirth: A systematic review. *CMAJ* **2008**, *178*, 165–172. [[CrossRef](#)] [[PubMed](#)]
2. Mathews, T.J.; Hamilton, B.E. Mean Age of Mothers is on the Rise: United States, 2000–2014. *NCHS Data Brief* **2016**, *232*, 1–8.
3. OECD Family Database. The Structure of Families 2.3: Age of Mothers at Childbirth and Age-Specific Fertility. 2019. Available online: <http://www.oecd.org/social/family/database.htm> (accessed on 18 September 2020).
4. Eurostat. Total Fertility Rate and Age of Women at Birth of First Child. Available online: [https://ec.europa.eu/eurostat/statistics-explained/index.php/Fertility\\_statistics](https://ec.europa.eu/eurostat/statistics-explained/index.php/Fertility_statistics) (accessed on 23 September 2020).
5. Maurer, R.R.; Foote, R.H. Maternal ageing and embryonic mortality in the rabbit. I. Repeated superovulation, embryo culture and transfer. *J. Reprod. Fertil.* **1971**, *25*, 329–341. [[CrossRef](#)]
6. Miller, P.B.; Charleston, J.S.; Battaglia, D.E.; Klein, N.A.; Soules, M.R. Morphometric analysis of primordial follicle number in pigtailed monkey ovaries: Symmetry and relationship with age. *Biol. Reprod.* **1999**, *61*, 553–556. [[CrossRef](#)] [[PubMed](#)]
7. Jones, K.P.; Walker, L.C.; Anderson, D.; Lacreuse, A.; Robson, S.L.; Hawkes, K. Depletion of ovarian follicles with age in chimpanzees: Similarities to humans. *Biol. Reprod.* **2007**, *77*, 247–251. [[CrossRef](#)] [[PubMed](#)]
8. Jolly, M.; Sebire, N.; Harris, J.; Robinson, S.; Regan, L. The risks associated with pregnancy in women aged 35 years or older. *Hum. Reprod.* **2000**, *15*, 2433–2437. [[CrossRef](#)] [[PubMed](#)]
9. Joseph, K.S.; Allen, A.C.; Dodds, L.; Turner, L.A.; Scott, H.; Liston, R. The perinatal effects of delayed childbearing. *Obstet. Gynecol.* **2005**, *105*, 1410–1418. [[CrossRef](#)]
10. Kenny, L.C.; Lavender, T.; McNamee, R.; O'Neill, S.M.; Mills, T.; Khashan, A.S. Advanced maternal age and adverse pregnancy outcome: Evidence from a large contemporary cohort. *PLoS ONE* **2013**, *8*, e56583. [[CrossRef](#)] [[PubMed](#)]
11. Hoffman, M.C.; Jeffers, S.; Carter, J.; Duthely, L.; Cotter, A.; González-Quintero, V.H. Pregnancy at or beyond age 40 years is associated with an increased risk of fetal death and other adverse outcomes. *Am. J. Obstet. Gynecol.* **2007**, *196*, e11–e13. [[CrossRef](#)]
12. Tatone, C. Oocyte senescence: A firm link to age-related female subfertility. *Gynecol. Endocrinol.* **2008**, *24*, 59–63. [[CrossRef](#)]
13. Tatone, C.; Amicarelli, F.; Carbone, M.C.; Monteleone, P.; Caserta, D.; Marci, R.; Artini, P.G.; Piomboni, P.; Focarelli, R. Cellular and molecular aspects of ovarian follicle ageing. *Hum. Reprod. Update* **2008**, *14*, 131–142. [[CrossRef](#)]
14. Byun, K.; Yoo, Y.; Son, M.; Lee, J.; Jeong, G.-B.; Park, Y.M.; Salekdeh, G.H.; Lee, B. Advanced glycation end-products produced systemically and by macrophages: A common contributor to inflammation and degenerative diseases. *Pharmacol. Ther.* **2017**, *177*, 44–55. [[CrossRef](#)] [[PubMed](#)]
15. Bellier, J.; Nokin, M.-J.; Lardé, E.; Karoyan, P.; Peulen, O.; Castronovo, V.; Bellahcène, A. Methylglyoxal, a potent inducer of AGEs, connects between diabetes and cancer. *Diabetes Res. Clin. Pract.* **2019**, *148*, 200–211. [[CrossRef](#)] [[PubMed](#)]
16. Muronetz, V.I.; Melnikova, A.K.; Seferbekova, Z.N.; Barinova, K.V.; Schmalhausen, E.V. Glycation, Glycolysis, and Neurodegenerative Diseases: Is There Any Connection? *Biochem. Mosc.* **2017**, *82*, 874–886. [[CrossRef](#)] [[PubMed](#)]
17. Mano, J. Reactive carbonyl species: Their production from lipid peroxides, action in environmental stress, and the detoxification mechanism. *Plant Physiol. Biochem.* **2012**, *59*, 90–97. [[CrossRef](#)]
18. Thornalley, P.J. Protein and nucleotide damage by glyoxal and methylglyoxal in physiological systems—role in ageing and disease. *Drug Metabol. Drug Interact.* **2008**, *23*, 125–150. [[CrossRef](#)]
19. Peppas, M.; Uribarri, J.; Vlassara, H. Aging and glycoxidant stress. *Hormones* **2008**, *7*, 123–132. [[CrossRef](#)]
20. Shipanova, I.N.; Glomb, M.A.; Nagaraj, R.H. Protein modification by methylglyoxal: Chemical nature and synthetic mechanism of a major fluorescent adduct. *Arch. Biochem. Biophys.* **1997**, *344*, 29–36. [[CrossRef](#)]
21. Thornalley, P.J. Glyoxalase I—Structure, function and a critical role in the enzymatic defence against glycation. *Biochem. Soc. Trans.* **2003**, *31*, 1343–1348. [[CrossRef](#)]
22. Kuhla, B.; Boeck, K.; Lüth, H.-J.; Schmidt, A.; Weigle, B.; Schmitz, M.; Ogunlade, V.; Münch, G.; Arendt, T. Age-dependent changes of glyoxalase I expression in human brain. *Neurobiol. Aging* **2006**, *27*, 815–822. [[CrossRef](#)]



23. Shinohara, M.; Thornalley, P.J.; Giardino, I.; Beisswenger, P.; Thorpe, S.R.; Onorato, J.; Brownlee, M. Overexpression of glyoxalase-I in bovine endothelial cells inhibits intracellular advanced glycation endproduct formation and prevents hyperglycemia-induced increases in macromolecular endocytosis. *J. Clin. Investig.* **1998**, *101*, 1142–1147. [[CrossRef](#)] [[PubMed](#)]
24. Thornalley, P.J. The glyoxalase system in health and disease. *Mol. Asp. Med.* **1993**, *14*, 287–371. [[CrossRef](#)]
25. Tatone, C.; Carbone, M.C.; Campanella, G.; Festuccia, C.; Artini, P.G.; Talesa, V.; Focarelli, R.; Amicarelli, F. Female reproductive dysfunction during ageing: Role of methylglyoxal in the formation of advanced glycation endproducts in ovaries of reproductively-aged mice. *J. Biol. Regul. Homeost. Agents* **2010**, *24*, 63–72. [[PubMed](#)]
26. Merhi, Z. Advanced glycation end products and their relevance in female reproduction. *Hum. Reprod.* **2014**, *29*, 135–145. [[CrossRef](#)]
27. Sauer, M.V. Reproduction at an advanced maternal age and maternal health. *Fertil. Steril.* **2015**, *103*, 1136–1143. [[CrossRef](#)]
28. Haucke, E.; Navarrete Santos, A.; Simm, A.; Henning, C.; Glomb, M.A.; Gürke, J.; Schindler, M.; Fischer, B.; Navarrete Santos, A. Accumulation of advanced glycation end products in the rabbit blastocyst under maternal diabetes. *Reproduction* **2014**, *148*, 169–178. [[CrossRef](#)]
29. Seeling, T.; Haucke, E.; Navarrete Santos, A.; Grybel, K.J.; Gürke, J.; Pendzialek, S.M.; Schindler, M.; Simm, A.; Navarrete Santos, A. Glyoxalase 1 expression is downregulated in preimplantation blastocysts of diabetic rabbits. *Reprod. Domest. Anim.* **2019**, *54* (Suppl. S3), 4–11. [[CrossRef](#)]
30. Fischer, B.; Chavatte-Palmer, P.; Viebahn, C.; Navarrete Santos, A.; Duranthon, V. Rabbit as a reproductive model for human health. *Reproduction* **2012**, *144*, 1–10. [[CrossRef](#)]
31. Navarrete Santos, A.; Augustin, R.; Lazzari, G.; Galli, C.; Sreenan, J.M.; Fischer, B. The insulin-dependent glucose transporter isoform 4 is expressed in bovine blastocysts. *Biochem. Biophys. Res. Commun.* **2000**, *271*, 753–760. [[CrossRef](#)]
32. Tonack, S.; Fischer, B.; Navarrete Santos, A. Expression of the insulin-responsive glucose transporter isoform 4 in blastocysts of C57/BL6 mice. *Anatomy Embryol.* **2004**, *208*, 225–230. [[CrossRef](#)]
33. Pendzialek, S.M.; Knelangen, J.M.; Schindler, M.; Gürke, J.; Grybel, K.J.; Gocza, E.; Fischer, B.; Navarrete Santos, A. Trophoblastic microRNAs are downregulated in a diabetic pregnancy through an inhibition of Drosha. *Mol. Cell. Endocrinol.* **2019**, *480*, 167–179. [[CrossRef](#)] [[PubMed](#)]
34. Pendzialek, S.M.; Schindler, M.; Plösch, T.; Gürke, J.; Haucke, E.; Hecht, S.; Fischer, B.; Santos, A.N. Cholesterol metabolism in rabbit blastocysts under maternal diabetes. *Reprod. Fertil. Dev.* **2017**, *29*, 1921–1931. [[CrossRef](#)]
35. Bélanger, M.; Yang, J.; Petit, J.-M.; Laroche, T.; Magistretti, P.J.; Allaman, I. Role of the glyoxalase system in astrocyte-mediated neuroprotection. *J. Neurosci.* **2011**, *31*, 18338–18352. [[CrossRef](#)]
36. Arai, M.; Nihonmatsu-Kikuchi, N.; Itokawa, M.; Rabbani, N.; Thornalley, P.J. Measurement of glyoxalase activities. *Biochem. Soc. Trans.* **2014**, *42*, 491–494. [[CrossRef](#)] [[PubMed](#)]
37. Kandaraki, E.; Chatzigeorgiou, A.; Piperi, C.; Palioura, E.; Palimeri, S.; Korkolopoulou, P.; Koutsilieris, M.; Papavassiliou, A.G. Reduced ovarian glyoxalase-I activity by dietary glycotoxins and androgen excess: A causative link to polycystic ovarian syndrome. *Mol. Med.* **2012**, *18*, 1183–1189. [[CrossRef](#)] [[PubMed](#)]
38. Stratmann, B.; Goldstein, B.; Thornalley, P.J.; Rabbani, N.; Tschoepe, D. Intracellular Accumulation of Methylglyoxal by Glyoxalase 1 Knock Down Alters Collagen Homeostasis in L6 Myoblasts. *Int. J. Mol. Sci.* **2017**, *18*, 480. [[CrossRef](#)] [[PubMed](#)]
39. Nigro, C.; Leone, A.; Longo, M.; Prevezano, I.; Fleming, T.H.; Nicolò, A.; Parrillo, L.; Spinelli, R.; Formisano, P.; Nawroth, P.P.; et al. Methylglyoxal accumulation de-regulates HoxA5 expression, thereby impairing angiogenesis in glyoxalase 1 knock-down mouse aortic endothelial cells. *Biochim. Biophys. Acta Mol. Basis Dis.* **2019**, *1865*, 73–85. [[CrossRef](#)]
40. Vannuccini, S.; Clifton, V.L.; Fraser, I.S.; Taylor, H.S.; Critchley, H.; Giudice, L.C.; Petraglia, F. Infertility and reproductive disorders: Impact of hormonal and inflammatory mechanisms on pregnancy outcome. *Hum. Reprod. Update* **2016**, *22*, 104–115. [[CrossRef](#)]
41. Diamanti-Kandaraki, E.; Piperi, C.; Patsouris, E.; Korkolopoulou, P.; Panidis, D.; Pawelczyk, L.; Papavassiliou, A.G.; Duleba, A.J. Immunohistochemical localization of advanced glycation end-products (AGEs) and their receptor (RAGE) in polycystic and normal ovaries. *Histochem. Cell Biol.* **2007**, *127*, 581–589. [[CrossRef](#)]

42. Papachroni, K.K.; Piperi, C.; Levidou, G.; Korkolopoulou, P.; Pawelczyk, L.; Diamanti-Kandarakis, E.; Papavassiliou, A.G. Lysyl oxidase interacts with AGE signalling to modulate collagen synthesis in polycystic ovarian tissue. *J. Cell. Mol. Med.* **2010**, *14*, 2460–2469. [[CrossRef](#)]
43. Tatone, C.; Amicarelli, F. The aging ovary—The poor granulosa cells. *Fertil. Steril.* **2013**, *99*, 12–17. [[CrossRef](#)] [[PubMed](#)]
44. Matsumine, M.; Shibata, N.; Ishitani, K.; Kobayashi, M.; Ohta, H. Pentosidine accumulation in human oocytes and their correlation to age-related apoptosis. *Acta Histochem. Cytochem.* **2008**, *41*, 97–104. [[CrossRef](#)] [[PubMed](#)]
45. Di Emidio, G.; Santini, S.J.; D’Alessandro, A.M.; Vetuschi, A.; Sferra, R.; Artini, P.G.; Carta, G.; Falone, S.; Amicarelli, F.; Tatone, C. SIRT1 participates in the response to methylglyoxal-dependent glycativ stress in mouse oocytes and ovary. *Biochim. Biophys. Acta Mol. Basis Dis.* **2019**, *1865*, 1389–1401. [[CrossRef](#)] [[PubMed](#)]
46. Wang, S.; He, G.; Chen, M.; Zuo, T.; Xu, W.; Liu, X. The Role of Antioxidant Enzymes in the Ovaries. *Oxid. Med. Cell. Longev.* **2017**, *2017*, 4371714. [[CrossRef](#)]
47. Al-Gubory, K.H.; Bolifraud, P.; Garrel, C. Regulation of key antioxidant enzymatic systems in the sheep endometrium by ovarian steroids. *Endocrinology* **2008**, *149*, 4428–4434. [[CrossRef](#)]
48. ProteinSimple. Simple Western Assays: Immunoassay. Available online: [https://www.proteinsimple.com/simple\\_western\\_assays.html](https://www.proteinsimple.com/simple_western_assays.html) (accessed on 18 September 2020).

**Publisher’s Note:** MDPI stays neutral with regard to jurisdictional claims in published maps and institutional affiliations.



© 2020 by the authors. Licensee MDPI, Basel, Switzerland. This article is an open access article distributed under the terms and conditions of the Creative Commons Attribution (CC BY) license (<http://creativecommons.org/licenses/by/4.0/>).